# Design and Synthesis of Novel Single-Crystalline Hierarchical CdS Nanostructures Generated by Thermal Evaporation Processes

**ARTICLE** *in* CRYSTAL GROWTH & DESIGN · APRIL 2011

Impact Factor: 4.89 · DOI: 10.1021/cg101463r



**5 AUTHORS**, INCLUDING:

Zai-Xing Yang
Nanjing University
**24** PUBLICATIONS **183** CITATIONS
SEE PROFILE

Chak Tong Au
Hong Kong Baptist University
**410** PUBLICATIONS **7,765** CITATIONS
SEE PROFILE

CRYSTAL GROWTH & DESIGN

ARTICLE

pubs.acs.org/crystal

# Design and Synthesis of Novel Single-Crystalline Hierarchical CdS Nanostructures Generated by Thermal Evaporation Processes

Zai-Xing Yang,[†] Wei Zhong,[†,*] Yu Deng,[†] Chak-Tong Au,[‡] and You-Wei Du[†]

[†]Nanjing National Laboratory of Microstructures and Department of Physics, Nanjing University, Nanjing 210093, People's Republic of China

[‡]Chemistry Department, Hong Kong Baptist University, Hong Kong, People's Republic of China

**ABSTRACT:** Through thermal evaporation of a mixture of CdS and graphite powder, we produced a novel hierarchical nanostructure of single-crystalline CdS. It is in the form of cuspidated double headed nanocomb. In the absence of graphite powder, the thermal evaporation of powder CdS alone would result in the formation of CdS nanobelts. The hexagonal wurtzite phase of the CdS nanostructures was verified by XRD, and the single crystallinity confirmed by SAED. As revealed in FESEM and TEM analysis, the obtained hierarchical CdS nanocomb has 2-fold symmetry and the teeth grown perpendicular to the comb trunk are nanospikes of much smaller size. A mechanism for the growth of the hierarchical CdS nanocombs and CdS nanobelts has been described. In the study of optical properties of the CdS nanomaterials, we observed that the photoluminescence peak of CdS nanocombs showed a red-shift of ~7 nm in comparison to that of CdS nanobelts.

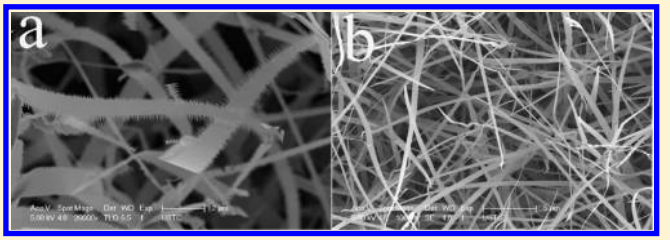


## INTRODUCTION

Motivated by their potential applications as building blocks for biosensors, as well as for optical and electronic devices, a variety of nanostructured single-crystalline semiconductors have been synthesized.[1−3] It was found that the unique physical and chemical properties of the materials are size- as well as shape-dependent.[4] In view of that, researchers turned their attention to the control synthesis of the materials in terms of architecture, size, morphology, and growth pattern of products. The goal is to tailor-make nanomaterials of specific properties for the fabrication of nanodevices.[5] For nanomaterials that are unique in hierarchical structures, they were investigated for application in areas such as field-effect transistors,[6] gas sensors,[7] photovoltaic devices,[8,9] electromechanical devices,[10] and scanning probe microscopy.[11]

It is hence meaningful to investigate the controlled generation of high-quality hierarchical nanostructures. So far, nanomaterials, such as brush-like ZnO,[12] flower-like $SnO_2$,[13] and comb-like ZnS[14] have been reported. Quantum dot-based hierarchical structures were also investigated.[15] Among semiconductors, CdS is one of the classics. With a direct band gap of 2.4 eV at room temperature (RT),[16] it is an excellent material for the fabrication of field emitters,[17] waveguides,[18] photoconductors,[19] logic gates,[20] and dye-sensitized solar cells.[21] In the past years, hierarchical nanostructures of CdS were prepared by a number of techniques. Using single-crystal ZnS nanowires as template and by a two-step evaporation technique, Zhou et al. produced high-quality CdS nanostructures of 6-fold symmetry.[22] On the other hand, through a TEPA-assisted solvothermal route involving the self-assembly of nanobelts and nanowires, Xiong et al. synthesized various kinds of novel networks of hierarchical CdS.[23] However, the two-step evaporation technique is difficult to control, and most of the organic solvents adopted in the solvothermal route are environment-unfriendly. It is hence valuable to develop a mild and simple route for the synthesis of hierarchical CdS nanomaterials.

In this article, we report a simple and environment-benign route to synthesize hierarchical CdS nanomaterials of high quality. Through a one-step low-pressure thermal evaporation of a mixture of CdS and graphite powder, we produced cuspidated double headed CdS nanocombs. For comparison purposes, we studied the CdS nanobelts generated through the same route but in the absence of graphite powder. It is worth pointing out that the approach is low-cost and the generation of product highly reproducible. To the best of our knowledge, the fabrication of such kind of hierarchical CdS nanomaterials using such an approach has never been reported before.

## EXPERIMENTAL SECTION

The process adopted for synthesis was similar to that of vapor−liquid−solid (VLS) technology. In short, a quartz tube (inner diameter = 50 mm; length = 700 mm) was installed in a tubular furnace. Then a ceramic boat loaded with a mixture of cadmium sulfide and graphite powder was placed at the center of the tube. Acting as substrates, pieces of Si(100) with the exposed face coated with gold (thickness = 15 nm) were placed downstream (12−18 cm from the center of the ceramic boat). Prior to heating, the quartz tube was purged with Ar at a flow rate of 20 sccm (standard cubic centimeters per minute) for 2 h. Then by means of a mechanical pump, the pressure inside the quartz tube was

**Received:** November 5, 2010
**Revised:** April 4, 2011
**Published:** April 18, 2011





dx.doi.org/10.1021/cg101463r | *Cryst. Growth Des.* 2011, 11, 2172–2176

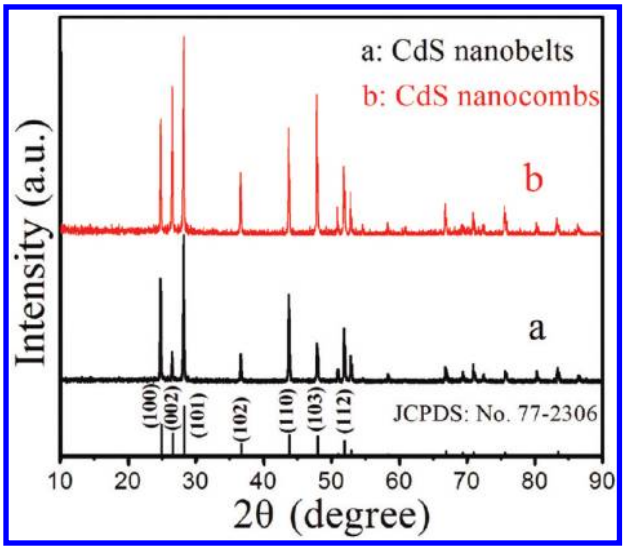


**Figure 1.** XRD pattern of (a) CdS nanobelts and (b) hierarchical nanocombs.

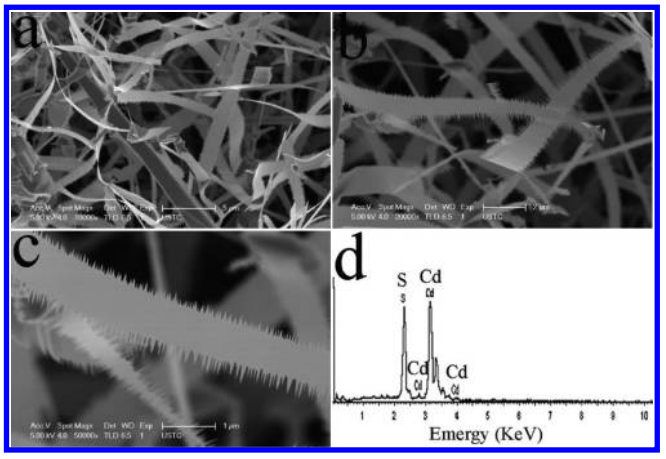


**Figure 2.** (a−c) FESEM images of the hierarchical CdS nanocombs at different magnifications. (d) EDS spectrum of the hierarchical CdS nanocombs.

maintained at ∼1.2 × $10^{-3}$ Pa, and the temperature was raised to 860 °C in a span of 1.5 h. After 2 h at 860 °C, the furnace was turned off. With the introduction of a flow of Ar, the quartz tube was cooled down to RT.

The materials formed on the Si(100) substrates were examined at RT for phase identification using an X-ray powder diffractometer (XRD; CuKα radiation; Model D/Max-RA, Rigaku). The morphology of samples was examined using a field emission scanning electron microscope (equipped with EDS) (FESEM; FEI Sirion 200, operated at an accelerating voltage of 5 kV) as well as a high-resolution transmission electron microscope (HRTEM) facilitated also for selected area electron diffraction (SAED) analysis (JEOL-2010, operated at an accelerating voltage of 200 kV). The optical properties of the materials were investigated for ultraviolet−visible (UV−vis) absorption (Cary, USA) and photoluminescence (PL, excitation source: He−Cd laser, 325 nm) at RT.

## RESULTS AND DISCUSSION

Figure 1 shows the typical XRD pattern of the products deposited on the Si substrates. The peaks are identical to those

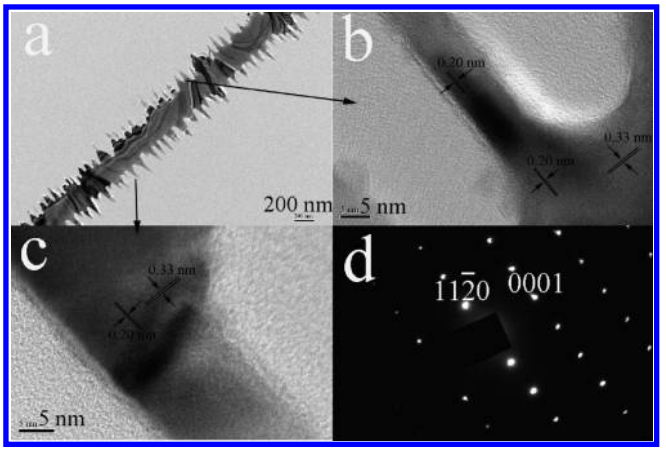


**Figure 3.** (a) TEM image of a strip of the hierarchical CdS nanocomb. (b, c) HRTEM images of selected spikes grown at the edges and (d) SAED image of the corresponding hierarchical CdS nanocomb.

of hexagonal wurtzite CdS, having $a$ = 0.4136 nm and $c$ = 0.6713 nm (JCPDS Card, No. 77-2306). Compared to that of JCPDS Card (No. 77−2306), the (002) peak in the XRD profile of the hierarchical CdS nanocombs is protruding, indicating preferential growth along the ⟨002⟩ direction. In the case of nanobelts, the (101) peak is protruding, indicating preferential growth along the ⟨101⟩ direction. The deduction based on the XRD results is in line with that based on the HRTEM (described in later section). The phase purity of CdS is high because there is no indication of the presence of other phases such as those of CdO, Cd, S, and C.

The FESEM technique can provide information related to the morphology of an entity without having its original nature disturbed. As shown in the FESEM image of Figure 2a, the product obtained in the thermal evaporation of a mixture of CdS and graphite powder is a collection of strips that are several tens of micrometers in length. Meanwhile, one can see that the obtained strips were harvested in large quantity, suggesting that the CdS strips were prepared in high purity and were not coated with amorphous materials. At high-magnification (Figures 2b and 2c), one can see sharp ends of the strips, and there are sharp spikes grown at the strip trunk. Loosely speaking, the hierarchical nanostructure can be considered as 2-fold in terms of symmetry. The surface of the strips is smooth, and the width of the strips decreases gradually from an average value of around 1.5 $\mu$m to a sharp end. With such an appearance, the nanomaterials are named as cuspidated double headed nanocombs. The EDS results show a Cd:S atomic ratio of 1:1 (Figure 2d), in accord with the stoichiometry of CdS.

Shown in Figure 3a is a typical TEM image of a strip of cuspidated double headed CdS nanocombs. The body of the nanocomb looks like a saw with teeth about 200 nm in length. The growth direction of the teeth is perpendicular to the comb trunk. This is in line with the results of FESEM investigation. However, the width of the comb is around 400 nm, much smaller than the average value (1.5 $\mu$m) detected in FESEM investigation. It could be because what is seen in Figure 3a is a section that is close to the sharp end. Shown in Figures 3b and 3c are the HRTEM images of selected teeth grown at the edges. They confirm the single crystallinity of the hierarchical CdS nanocombs, and one can detect lattice spacing of 0.33 and 0.20 nm assignable to (0001) and (11$\bar{2}$0) planes, respectively. The SAED pattern of Figure 3d further confirms the single crystallinity of the hierarchical CdS


dx.doi.org/10.1021/cg101463r |*Cryst. Growth Des.* 2011, 11, 2172–2176

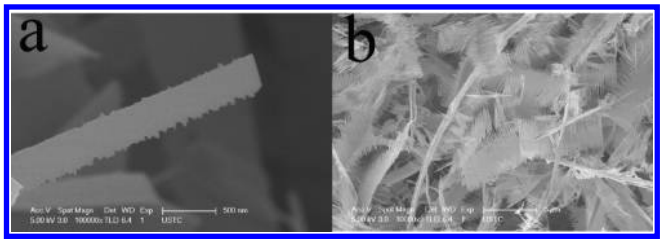


**Figure 4.** FESEM images of samples obtained at deposition time of (a) 1 h and (b) 3 h.

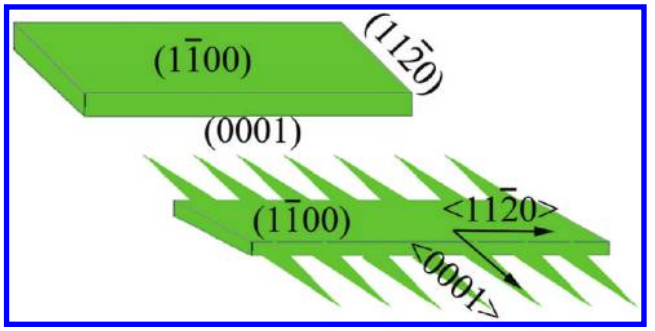


**Figure 5.** Schematics of CdS nanobelt and hierarchical nanocomb.

nanocombs. Nonetheless, as shown in Figures 3b and 3c, the spikes at the edges are poor in crystallinity. Overall the results suggest that the body of the comb grows along the ⟨110⟩ direction, while the teeth along the ⟨001⟩ direction.

We found that the length of the teeth of the hierarchical CdS nanocombs could be controlled by simply varying the time of synthesis. Shown in Figure 4 are the FESEM images of samples collected at a deposition time of 1 and 3 h. At 1 h, the length of the teeth is about 50 nm (Figure 4a). When the deposition time reaches 3 h, the length of the saw-like entity is up to micrometer scale. In other words, the double headed nanocombs that are tens of micrometers in length can be formed using the adopted synthetic method (Figure 4b).

Shown in Figure 5 are sketches of CdS nanobelt and hierarchical nanocomb. On the basis of the results of TEM and time-dependent FESEM investigation, it is reasonable to hypothesize that the hierarchical CdS nanocombs are formed using CdS nanobelts as template. Compared to the step of CdS nucleation, the deposition of CdS molecules on an existing nanostructure is more favorable, and the net result is the growth of the nanostructure.[6] The top and bottom surfaces of CdS nanobelts and hierarchical nanocombs are (1$\bar{1}$00) in orientation whereas the orientations of the side planes along the length and breadth are (0001) and (11$\bar{2}$0), respectively. As far as the growth direction of a strip of CdS is concerned, ⟨10$\bar{1}$0⟩ and ⟨0001⟩ are preferred.[24−26] However, under specific conditions or when a VLS mechanism is applicable, ⟨10$\bar{1}$0⟩ and ⟨0001⟩ are not preferred. For example, Wang et al. synthesized CdS nanowires through thermal evaporation of CdS powders under controlled conditions over Au catalyst, and the growth direction of nanowires was ⟨131⟩.[27] In the presence of graphite powder, the growth of the nanocombs is along the ⟨11$\bar{2}$0⟩ direction while that of nanospikes along the ⟨0001⟩ direction. Apparently, the growth rate along the former is faster than that along the latter, and there is the development of sharp spikes at the edges.

The role of graphite should be similar to that when it was used in the catalytic growth of ZnO nanowires through vapor

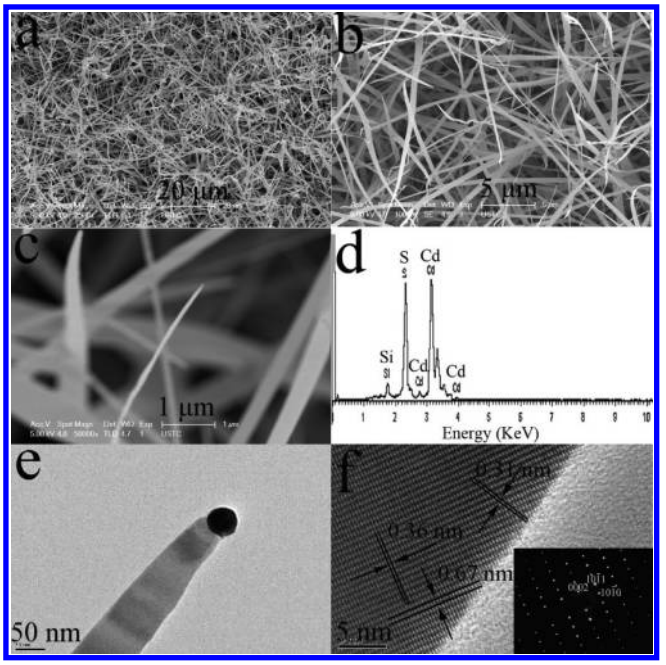


**Figure 6.** (a−c) FESEM images and (d) EDS spectrum of CdS nanobelts. (e) TEM image of a CdS nanobelt. (f) HRTEM image of CdS nanobelt (inset is the corresponding SAED pattern).

transportation.[28] Under the adopted conditions, CdS is reduced by carbon into Cd according to the following reactions:

$$2\mathrm{CdS(solid)} + \mathrm{C} \rightarrow 2\mathrm{Cd(gas)} + \mathrm{CS_2} \quad (1)$$

$$\mathrm{C} + \mathrm{CS_2} \rightarrow 2\mathrm{CS} \quad (2)$$

$$\mathrm{CdS(solid)} + \mathrm{CS} \rightarrow \mathrm{Cd(gas)} + \mathrm{CS_2} \quad (3)$$

Carried by the Ar flow, the Cd vapor was transported to the silicon substrates and reacted with the Au catalyst at a lower temperature to form alloy droplets. As the droplets became supersaturated with Cd, there was the generation of crystalline CdS nanostrips, plausibly according to reaction 4 below:

$$\mathrm{Cd(dissolved\ in\ Au)} + \mathrm{CS_2} \rightarrow \mathrm{CdS} + \mathrm{CS} \quad (4)$$

This is an exothermic step and the formation of CdS nanostrips is favored with the lowering of temperature. As described before, the CdS growth rate on CdS surfaces of different orientations are unequal. As a result, there is the generation of the saw-like nanostructure.

In the control experiment without graphite, CdS nanobelts became the major product (Figure 6). From the FESEM, TEM, EDS, and SAED results, one can see that single-crystalline CdS in the form of nanobelt is produced in abundance. As shown in Figures 6b and 6c, the length of the belts could be up to several tens of micrometers; one can also spot sharp tips at the ends of the belts. The EDS results (Figure 6d, Si signal is due to the Si substrate) suggest a Cd:S atomic ratio of 1:1. The TEM image of Figure 6e shows that there is the presence of a nanoparticle at the end of the CdS nanobelt. The HRTEM image (Figure 6f) and the corresponding SAED pattern (inset of Figure 6f) indicate the grow direction (along ⟨101⟩) and crystallinity of the CdS nanobelts. Furthermore, one can see *d*-spacing of 0.36, 0.67, and 0.31 nm corresponding to (100), (001) and (101) planes of


dx.doi.org/10.1021/cg101463r |*Cryst. Growth Des.* 2011, 11, 2172–2176

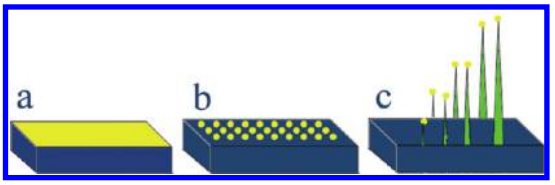


**Figure 7.** Growth process of CdS nanobelts.

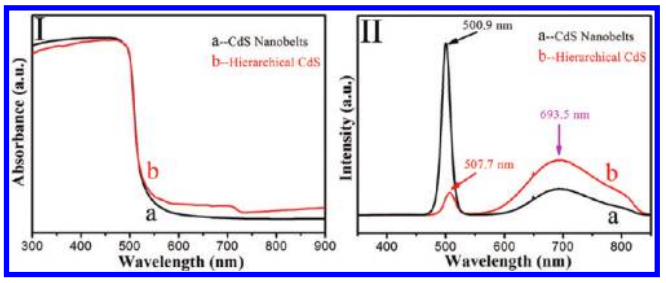


**Figure 8.** (I) UV−vis absorption and (II) PL spectra of (a) CdS nanobelts and (b) hierarchical nanocombs.

CdS, respectively, reflecting the single-crystal hexagonal wurtzite nature of the material.

On the basis of the results of Figures 6c and 6e, we deduce that the nanoparticle is made up of gold, and the growth of CdS nanobelt follows the VLS mechanism. As shown in Figure 7, at high enough temperature the Au catalyst melted and became small liquid droplets. With the evaporation of CdS, CdS vapor was carried toward the gold droplets by the Ar flow. When the gold droplets were supersaturated with CdS, there was the precipitation of CdS at the Au/Si interface. The continuous precipitation of CdS and growth of CdS crystal would result in the formation of CdS nanobelts with a gold droplet resting at the end of the belts.

We studied the optical properties of CdS nanobelts and hierarchical nanocombs. Figure 8I shows the UV−vis spectra of the samples. Both samples show absorption at ∼480 nm, which is blue-shifted compared to that of bulk CdS (513 nm),[29] suggesting the presence of quantum size effect. The absorption tail in the case of the hierarchical CdS nanocombs is due to scattering by the crystals.[30] Shown in Figure 8II is the PL spectra of CdS nanobelts and hierarchical nanocombs. In the former case (Figure 8IIa), the intense peak at ∼501 nm is due to the near-band-edge emission of CdS. A broad emission band of lower intensity centered at ∼693 nm is also recorded; such a band is often connected with structure defects, ionized vacancies, or impurities.[31,32] It is easier to yield sulfur vacancies in CdS materials because the radius of $S^{2-}$ is smaller than that of $Cd^{2+}$.[33] On the basis of the results of Wang at el., the defect emission contributing to 693 nm emission may be attributed to the high density of sulfur vacancies in CdS nanostructures.[34−36] Being high in crystallinity and perfect in belt-like morphology, the CdS nanobelts are low in structure defect, ionized vacancy, and impurity, showing strong near-band-edge emission at 501 nm and weak emission at 693 nm. In the PL spectrum of the hierarchical CdS nanocombs, there are two intense peaks centered at ∼508 and ∼693 nm; the intensity of the former (due to near-band-edge emission) is much lower than that of the latter (Figure 8IIb). Because of the presence of spikes at the edges, the hierarchical CdS nanocombs are lower in crystallinity than nanobelts (Figures 3b and 3c), and have a large amount of defect states. Being richer in structure defect and sulfur vacancies, the sample shows an emission at 693 nm stronger than the near-band-edge emission.[34] It is noted that the near-band-edge emission of the hierarchical CdS nanocombs shows a red shift of ∼7 nm in comparison to that of CdS nanobelts, plausibly due to shape- and/or size-effect. The unique properties of CdS nanobelts and hierarchical nanocombs suggest that they can be utilized in the industry of optoelectronic nanodevices.

## CONCLUSIONS

Cuspidated double headed CdS nanocombs were synthesized by simple thermal evaporation of a mixture of CdS and graphite powder at low pressure. It was observed that without graphite, CdS nanobelts would be the major product. It is clear that in the VLS process for the formation of hierarchical CdS nanocombs, graphite has a crucial role to play. It was found that compared to the PL peak of CdS nanobelts, that of hierarchical CdS nanocombs red-shifted by ∼7 nm. These unique properties of the hierarchical CdS nanocombs and CdS nanobelts suggest that they can be utilized in the industry of optoelectronic nanodevices.

## AUTHOR INFORMATION

### Corresponding Author

*Tel: +86-25-83621200. Fax: +86-25-83595535. E-mail: wzhong@mail.nju.edu.cn.

## ACKNOWLEDGMENT

We would like to thank the Foundation of the National Key Project for Basic Research (Grant Nos. 2011CB922102 and 2010CB923402), National Laboratory of Solid State Microstructures, Nanjing University (Grant No. 2010ZZ18), and Discipline Crossing Foundation of Nanjing University, People's Republic of China, for financial support.

## REFERENCES

(1) Lu, W.; Lieber, C. M. *Nat. Mater.* **2007**, *6*, 841.
(2) Yang, Z. X.; Zhong, W.; Au, C. T.; Du, X.; Song, H. A.; Qi, X. S.; Ye, X. J.; Xu, M. H.; Du, Y. W. *J. Phys. Chem. C* **2009**, *113*, 21269.
(3) Biju, V.; Itoh, T.; Ishikawa, M. *Chem. Soc. Rev.* **2010**, *39*, 3031.
(4) Watt, J.; Young, N.; Haigh, S.; Kirkland, A.; Tilley, R. D. *Adv. Mater.* **2009**, *21*, 2288.
(5) Ghoshal, T.; Biswas, S.; Nambissan, P. M. G.; Majumdar, G.; De, S. K. *Cryst. Growth Des.* **2009**, *9*, 1287.
(6) Zhang, M.; Zhai, T. Y.; Wang, X.; Ma, Y.; Yao, J. N. *Cryst. Growth Des.* **2010**, *10*, 1201.
(7) Jiang, L. Y.; Wu, X. L.; Guo, Y. G.; Wan, L. J. *J. Phys. Chem. C* **2009**, *113*, 14213.
(8) Zhou, Y.; Li, Y. C.; Zhong, H. Z.; Hou, J. H.; Ding, Y. Q.; Yang, C. H.; Li, Y. F. *Nanotechnology* **2006**, *17*, 4041.
(9) Zhong, H. Z.; Zhou, Y.; Yang, Y.; Yang, C. H.; Li, Y. F. *J. Phys. Chem. C* **2007**, *111*, 6538.
(10) Fang, L.; Park, J. Y.; Cui, Y.; Alivisatos, P.; Shcrier, J.; Lee, B.; Wang, L. W.; Salmeron, M. *J. Chem. Phys.* **2007**, *127*, 184704.
(11) Nobile, C.; Ashby, P. D.; Schuck, P. J.; Fiore, A.; Mastria, R.; Cingolani, R.; Manna, L.; Krahne, R. *Small* **2008**, *4*, 2123.
(12) Lao, J. Y.; Wen, J. G.; Ren, Z. F. *Nano Lett.* **2002**, *2*, 1287.
(13) Li, Z. R.; Li, X. L.; Zhang, X. X.; Qian, Y. T. *J. Cryst. Growth* **2006**, *291*, 258.
(14) Ma, C.; Moore, D.; Li, J.; Wang, Z. L. *Adv. Mater.* **2003**, *15*, 228.

(15) Biju, V.; Itoh, T.; Baba, Y.; Ishikawa, M. *J. Phys. Chem. B* **2006**, *110*, 26068.
(16) Shen, G.; Cho, J. H.; Yoo, J. K.; Yi, G. C.; Lee, C. J. *J. Phys. Chem. B* **2005**, *109*, 9294.
(17) Li, L.; Wu, P. C.; Fang, X. S.; Zhai, T. Y.; Dai, L.; Liao, M. Y. *Adv. Mater.* **2010**, *22*, 3161.
(18) Agarwal, R.; Barrelet, C. J.; Lieber, C. M. *Nano Lett.* **2005**, *5*, 917.
(19) Gao, T.; Li, Q. H.; Wang, T. H. *Appl. Phys. Lett.* **2005**, *86*, 173105.
(20) Ma, R. M.; Dai, L.; Huo, H. B.; Xu, W. J.; Oin, G. G. *Nano Lett.* **2007**, *7*, 3300.
(21) Fan, Z. Y.; Razavi, H.; Do, J.; Moriwaki, A.; Ergen, O.; Chueh, Y.; Leu, P. W.; Ho, J. C.; Takahashi, T.; Reichertz, L. A.; Neale, S.; Yu, K.; Wu, M.; Ager, J. W.; Javey, A. *Nat. Mater.* **2009**, *8*, 648.
(22) Zhou, W. C.; Pan, A. L.; Li, Y.; Dai, G. Z.; Wan, Q.; Zhang, Q. L.; Zou, B. S. *J. Phys. Chem. C* **2008**, *112*, 9253.
(23) Xiong, S. L.; Zhang, X. G.; Qian, Y. T. *Cryst. Growth Des.* **2009**, *9*, 5259.
(24) Zhai, T. Y.; Gu, Z. J.; Zhong, H. Z.; Dong, Y.; Ma, Y.; Fu, H. B.; Li, Y. F.; Yao, J. N. *Cryst. Growth Des.* **2007**, *7*, 488.
(25) Dong, L. F.; Jiao, J.; Coulter, M.; Love, L. *Chem. Phys. Lett.* **2003**, *376*, 653.
(26) Chen, S. T.; Zhang, X. L.; Zhang, Q. H.; Tan, W. H. *Nanoscale Res. Lett.* **2009**, *4*, 1159.
(27) Wang, Y. W.; Meng, G. W.; Zhang, L. D.; Liang, C. H.; Zhang, J. *Chem. Mater.* **2002**, *14*, 1773.
(28) Huang, M. H.; Wu, Y. Y.; Feick, H.; Tran, N.; Weber, E.; Yang, P. D. *Adv. Mater.* **2001**, *13*, 113.
(29) Weller, H. *Angew. Chem., Int. Ed.* **1993**, *32*, 41.
(30) Nanda, J.; Sapra, S.; Sarma, D. D. *Chem. Mater.* **2000**, *12*, 1018.
(31) Ge, J. P.; Li, Y. D. *Adv. Funct. Mater.* **2004**, *14*, 157.
(32) Gao, F.; Lu, Q. Y.; Xie, S. H.; Zhao, D. Y. *Adv. Mater.* **2002**, *14*, 1537.
(33) Cao, H. Q.; Wang, G. Z.; Zhang, S. C.; Zhang, X. R.; Rabinovich, D. *Inorg. Chem.* **2006**, *45*, 5103.
(34) Wang, X. L.; Feng, Z. C.; Fan, D. Y.; Fan, F. T.; Li, C. *Cryst. Growth Des.* **2010**, *10*, 5312.
(35) Xu, L.; Su, Y.; Cai, D.; Chen, Y. Q.; Feng, Y. *Mater. Lett.* **2006**, *60*, 1420.
(36) Uchihara, T.; Kato, H.; Miyagi, E. *J. Photochem. Photobiol. A* **2006**, *181*, 86.